A Simple Discrete-time Tracking Differentiator and Its Application to Speed and Position Detection System for a Maglev Train

Hehong Zhang, Yunde Xie, Gaoxi Xiao, Chao Zhai, and Zhiqiang Long

Abstract—In this brief, a novel tracking differentiator based on discrete time optimal control (DTOC) is presented. In particular, using the state back-stepping method, a DTOC law for a discrete-time, double-integral system is determined by linearized criterion, which equips the tracking differentiator with a simple structure. The analysis of the proposed tracking differentiator reveals its filtering mechanism. Simulation results show that it performs well in signal-tracking, differentiation acquisition and reducing the computation resources needed. Experiments on the speed and position detection system for a maglev train demonstrate that the proposed tracking differentiator group, with moving-average algorithm, can filter noises, amend distortion signals effectively and compensate for phase delays when the train is passing over track joints.

Index Terms—Tracking differentiator, discrete time, time optimal control, linearized criterion, filter, phase delay, maglev train.

I. INTRODUCTION

THE differentiation of a given signal in real time is a well-known yet challenging problem in control engineering and theory [1], [2]. The proportional-integral-derivative (PID) control law developed in the last century still plays an essential role in modern control engineering practice [3], [4]. However, since derivative signals are prone to be corrupted by noise and derivative control is usually not physically implementable, the PID control is usually degraded to PI control [5]. To deal with this, researchers have proposed many different approaches for differentiator design, including those based on a high-gain observer [6], a linear time-derivative tracker [7], a super-twisting second-order sliding mode algorithm [8], robust exact differentiation [9], [10], and a finite time convergent differentiator [11] etc.

First proposed by Han [12], a noise-tolerant time optimal control (TOC)-based tracking differentiator (TD) allows one to avoid a setpoint jump in the emerging active disturbance rejection controller. The advantage of this TD is that it sets a weak condition on the stability of the systems to be constructed for TD and requires a weak condition on the input. In addition, it also has the advantage of smoothness compared

Y. D. Xie is with Beijng Enterprises Holding Maglev Technology Development Company Limited, Beijing 10024, China. e-mail: xieyunde@outlook.com.

H. H. Zhang, C. Zhai and G. Xiao are with School of Electrical and Electronic Engineering, Nanyang Technological University, Singapore.

H. H. Zhang and Z. Q. Long are with College of Mechatronics Engineering and Automation, National University of Defense Technology, Changsha, China.

with the obvious chattering problem encountered by sliding-mode-based differentiators [13]. The following presents a brief outline for the construction of this TD:

The double-integral system is defined as

$$\begin{cases} \dot{x}_1 = x_2, \\ \dot{x}_2 = u, \quad |u| \leq r \end{cases} \tag{1}$$

where r is a constant. Note that, depending on the physical limitations in each application, the parameter r can be selected accordingly to speed up or slow down the transient profile. The resulting feedback control law that drives the state from any initial point to the origin in the shortest time is [14], [15]

$$u = -r\text{sign}(x_1 - v + \frac{x_2|x_2|}{2r}) \tag{2}$$

where v is the desired value for x_1. The switching curve function is $\Gamma(x_1, x_2) = x_1 + \frac{x_2|x_2|}{2r}$. Using this principle, we can obtain the desired trajectory and its derivative by solving the following differential equations:

$$\begin{cases} \dot{v}_1 = v_2, \\ \dot{v}_2 = -r\text{sign}(v_1 - v + \frac{v_2|v_2|}{2r}) \end{cases} \tag{3}$$

where v_1 is the desired trajectory and v_2 is its derivative.

With the developments in computer control technology, most control algorithms are now implemented in the discrete time domain. Direct digitization of a continuous TOC solution of (2) is problematic in practice because of the high-frequency chattering of the control signals [16]. This problem can be addressed by using a discrete-time solution for a discrete double-integral system $v_1(k + 1) = v_1(k) + hv_2(k)$, $v_2(k + 1) = v_2(k) + hu(k), |u(k)| \leq r$ to obtain $u = Fhan(v_1(k) - v(k), v_2(k), r_0, h_0)$, where h is the sampling period, and r_0 and h_0 are controller parameters [12], [16].

However, the discrete time optimal control (DTOC) law ($Fhan$) of the TD is determined by comparing the position of the initial state with the isochronic region obtained through non-linear boundary transformation. This makes the structure of a TD to be complex with non-linear calculations, including square-root calculations. In this brief, the mathematical derivation of a new closed-form discrete time optimal control law for discrete form of the system in (1) is presented. Unlike the control law $Fhan$, the DTOC law is based on a linearized criterion that depends upon the position of the initial state point on the phase plane. In doing so, the new control law has a simpler structure that is much easier to be applied in practical engineering scenarios. Experiments are carried out on position

signal processing for position sensing in the speed and position detection system of a maglev train [17], [18]. In practice, the signals from the position sensor may be aberrant due to track joints, which leads to low efficiency of the traction system and even safety misadventures. The proposed TD can be used to construct a TD group with a moving-average algorithm that filters the noises, compensates for phase delays, and amends distortion signals when the train is passing over track joints.

The paper is organized as follows: the new DTOC law is proposed in Section II. The structure of the TD and its filtering characteristic are discussed in Section III. In Section IV, numerical simulation results are presented to compare the performance of signal tracking, differentiation acquisition and the computation resources needed in field-programmable gate array (FPGA) application between the control law $Fhan$ and the proposed law, followed by experiment results on position signal processing for the speed and position detection system of a maglev train. Finally Section V concludes the paper.

II. DISCRETE TIME OPTIMAL CONTROL LAW

Consider a discrete-time double-integral system

$$x(k+1) = Ax(k) + Bu(k), |u(k)| \leq r \qquad (4)$$

where $A = \begin{pmatrix} 1 & h \\ 0 & 1 \end{pmatrix}$, $B = \begin{pmatrix} 1 \\ h \end{pmatrix}$ and $x(k) = [x_1(k), x_2(k)]^T$. The objective here is to derive a time optimal control (TOC) law directly in discrete time domain. The problem is defined as follows:

DTOC Law: Given the system (4) and its initial state $x(0)$, determine the control signal sequence, $u(0)$, $u(1)$,..., $u(k)$, such that the state $x(k)$ is driven back to the origin in a minimum and finite number of steps, subject to the constraint of $|u(k)| \leq r$. That is, find $u(k^*)$, $|u(k)| \leq r$, such that $k^* = \min \{k|x(k+1) = 0\}$.

In bang-bang control, the control signal switches between its two extreme values ($u = +r$ or $u = -r$) around the switching curve, and it switches the sign instantaneously after reaching the switching curve. For a discrete time system, however, the process of sign-switching occurs within a sampling period h. During that process, the corresponding state sequences remain in a certain region (denoted as Ω) near the switching curve. The control signals for the state sequences in region Ω are determined by a linearized criterion. The control signal varies from a certain positive (negative) value to a negative (positive) value when control signal u passes from one side of the region Ω to the other. All initial state sequences outside region Ω when the control signal takes an extreme value, i.e., $u = +r$ or $u = -r$, are located at certain curves, referred to as boundary curves Γ_A and Γ_B. Region Ω is surrounded by these boundary curves. In addition, when the value of the control signal varies in $[-r, r]$, there exists a state that corresponds to $u = 0$. All states that correspond to $u = 0$ constitute another curve, which is referred to as the control characteristic curve Γ_C.

In deriving the DTOC law, one must find the control signal sequence for any initial state point $x(0) \in \Omega$ or $x(0) \notin \Omega$. The whole task is divided into two parts:

I: Determine the boundary curves of region Ω and the control characteristic curve based on the state back-stepping approach, i.e., the representation of the initial condition $x(0) = [x_1(0), x_2(0)]^T$ in terms of h and r, from which the state can be driven back to the origin in $(k + 1)$ steps.

II: For any given initial condition $x(0) \in \Omega$ or $x(0) \notin \Omega$, find the corresponding control signal sequence.

A. Determination of the Boundary Curves and Control Characteristic Curve

For any initial state sequence, at least one admissible control sequence exists, e.g., $u(0)$, $u(1)$, ..., $u(k)$, that makes the solution to (4) satisfy $x(k+1) = 0$. Under the initial condition $x(0)$, the solution is

$$x(k + 1) = A^{k+1}x(0) + \sum_{i=0}^{k} A^{k-i}Bu(i) \qquad (5)$$

where $x(0) = [x_1(0), x_2(0)]^T$ and $i = 0, 1, 2, ..., k$. It manifests that $x(k + 1) = 0$. Therefore, the initial condition satisfies

$$x(0) = \sum_{i=0}^{k} \begin{pmatrix} (i+1)h^2 \\ -h \end{pmatrix} u(i) \qquad (6)$$

Adopting the state back-stepping approach (above), we can determine the two boundary curves Γ_A and Γ_B as well as the control characteristic curve Γ_C as follows:

To obtain the boundary curve Γ_A, we suppose that $\{a_{+k}\}$ and $\{a_{-k}\}$ are the sets of any $x(0)$ that can be driven back to the origin with the control signal sequence $u(i) = +r$ or $u(i) = -r$, $i = 0, 1, 2, ..., k$. For this we specify that all initial states in set $\{a_{+k}\}$ consist of Γ_A^+ and all initial states in set $\{a_{-k}\}$ consist of Γ_A^-.

For set $\{a_{+k}\}$, the following result holds when the control signal sequence takes on $u(i) = +r$ according to (6).

$$x(0) = r \sum_{i=0}^{k} \begin{pmatrix} (i+1)h^2 \\ -h \end{pmatrix} \qquad (7)$$

And we have: $x_1(0) = rh^2(\frac{k^2}{2} + \frac{3k}{2} + 1)$ and $x_2(0) = -rh(k+1) < 0$. Simplifying $x(0)$ into x and eliminating the variable k results in the boundary curve Γ_A^+, which is $x_1 = \frac{x_2^2}{2r} - \frac{1}{2}hx_2$, where $x_2 < 0$. Similarly, we can get the boundary curve Γ_A^-: $x_1 = -\frac{x_2^2}{2r} - \frac{1}{2}hx_2$, where $x_2 > 0$. Therefore, the entire boundary curve Γ_A (see Fig. 1) is

$$\Gamma_A : x_1 + \frac{x_2|x_2|}{2r} + \frac{1}{2}hx_2 = 0 \qquad (8)$$

We then determine the boundary curve Γ_B. If we suppose that $\{b_{+k}\}$ and $\{b_{-k}\}(k > 2)$ are the sets of any initial state $x(0)$ that can be driven back to the origin when the control signal takes on $u(0) = -r$ or $u(0) = +r$ in the first step, from then on the control sequence becomes $u(i) = +r$ or $u(i) = -r, i = 1, 2, ..., k$, respectively. Similarly, the boundary curve Γ_B consists of Γ_B^+ and Γ_B^-.

For set $\{b_{+k}\}$, the rule presented above for choosing the control signal sequence allows us to obtain $x_1 = rh^2(\frac{k^2}{2} + \frac{3k}{2} - 1)$ and $x_2 = -rh(k - 1) < 0$. Eliminating the variable
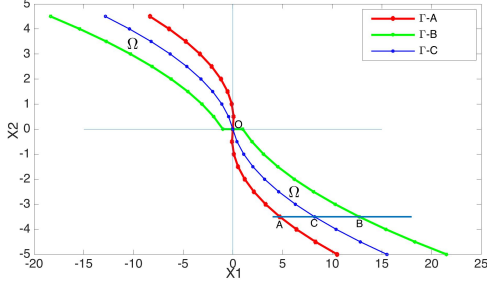
Fig. 1. Illustration of two boundary curves (Γ_A and Γ_B), control characteristic curve Γ_C, region Ω (surrounded by two boundary curves), and three intersection points A, B, and C.

Fig. 2. Illustration of two-step reachable region Ω_r, i.e., diamond region.

k, the boundary curve Γ_B^+ is $x_1 = \frac{x_2^2}{2r} - \frac{5}{2}hx_2 + h^2r$ and there exists $x_1 + hx_2 = \frac{1}{2}rh^2k(k+1) > 0$. Similarly, we can obtain the boundary curve Γ_B^-: $x_1 = -\frac{x_2^2}{2r} - \frac{5}{2}hx_2 - h^2r, x_1 + hx_2 < 0$. Therefore, the entire boundary curve Γ_B (see Fig. 1) is

$$\Gamma_B : x_1 - s\frac{x_2^2}{2r} + \frac{5}{2}hx_2 - sh^2r = 0 \qquad (9)$$

where $s = \text{sign}(x_1 + hx_2)$.

We finally determine the control characteristic curve Γ_C. If we suppose that $\{c_{+k}\}$ and $\{c_{-k}\}$ ($k > 2$) are the sets of any initial state $x(0)$ that can be driven back to the origin when the control signal takes on $u(0) = 0$ beginning in the first step, then the control sequence takes on $u(i) = +r$ or $u(i) = -r, i = 1, 2, ..., k$. Similarly, the boundary curve Γ_C consists of Γ_C^+ and Γ_C^-.

For set $\{c_{+k}\}$, there exists $x_1 = \frac{1}{2}rh^2(k^2 + 3k + 2)$ and $x_2 = -rhk < 0$ according to the rule for choosing the control signal sequence, as shown above. By eliminating the variable k, we have that the control characteristic curve Γ_C^+ is $x_1 = \frac{x_2^2}{2r} - \frac{3}{2}hx_2$. Similarly we can obtain the control characteristic curve Γ_C^-: $x_1 = -\frac{x_2^2}{2r} - \frac{3}{2}hx_2 - h^2r$. Therefore, the entire control characteristic curve Γ_C (see Fig. 1) is

$$\Gamma_C : x_1 + \frac{x_2|x_2|}{2r} + \frac{3}{2}hx_2 = 0 \qquad (10)$$

B. Construction of the DTOC Law

The new DTOC law is constructed based on the boundary curves and the control characteristic curve proposed above. As shown in Fig. 1, we denote that, for any initial state $M(x_1, x_2)$ in the fourth quadrant ($x_1 > 0, x_2 < 0$), an auxiliary line $x_2 = x_2(M)$ intersects with the boundary curves and the control characteristic curve at points A, C and B (in the direction of x_1). The coordinates of x_A, x_C, and x_B along the x-axis are

$$\begin{cases} x_A = \frac{x_2^2}{2r} + \frac{1}{2}h|x_2| \\ x_B = \frac{x_2^2}{2r} + +\frac{5}{2}h|x_2| + h^2r \\ x_C = \frac{x_2^2}{2r} + +\frac{3}{2}h|x_2|. \end{cases} \qquad (11)$$

For any initial state $M(x_1, x_2)$ satisfying $x_1 < x_A$ or $x_1 > x_B$, the control signal is taken as $u = +r$ or $u = -r$. For any
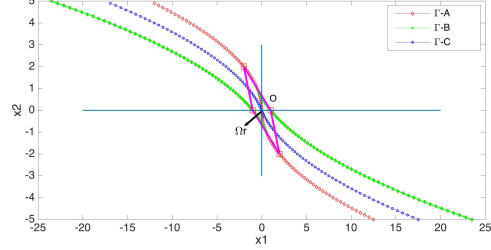
initial state $M(x_1, x_2)$ satisfying $x_1 \in [x_A, x_C]$, the control signal can be determined as follows:

$$u = -r\alpha\text{sign}(x_2) \qquad (12)$$

where $\alpha = \frac{x_C - x_1}{x_C - x_A}$. For any initial state $M(x_1, x_2)$ satisfying $x_1 \in [x_C, x_B]$, the control signal is calculated as:

$$u = r\beta\text{sign}(x_2) \qquad (13)$$

where $\beta = \frac{x_1 - x_C}{x_B - x_C}$.

When the initial state $M(x_1, x_2)$ is in the second quadrant, the control signal sequence can be constructed similarly. However, when the initial state $M(x_1, x_2)$ is in the first or third quadrant (located outside region Ω), two different cases have to be considered when selecting the control signal. When $M(x_1, x_2)$ cannot be driven back to the origin within two steps, that is, the initial state does not satisfy the condition $x_1^2 + x_2^2 = 0$, then $u = -r\text{sign}(x_1 + hx_2)$. When $M(x_1, x_2)$ can be driven back to the origin within two steps, the initial state $x(0)$ and the corresponding control signal sequence satisfy (6), i.e.,

$$\begin{cases} x_1(1) = x_1(0) + hx_2(0) \\ x_2(1) = x_2(0) + hu(0) \\ x_1(2) = x_1(1) + hx_2(1) \\ x_2(2) = x_2(1) + hu(1). \end{cases} \qquad (14)$$

Furthermore, when $M(x_1, x_2)$ can be driven back to the origin within two steps, the corresponding control signals can be derived as follows:

$$\begin{cases} u(0) = -\frac{x_1(0) + 2hx_2(0)}{h^2} \\ u(1) = \frac{x_1(0) + hx_2(0)}{h^2}. \end{cases} \qquad (15)$$

The condition $u(1) \leq r$ is a sufficient condition for driving the initial state back to the origin within two steps. When it is satisfied, the control signal can take on $u(0)$ and $u(1)$ in (15) to drive the initial state back to the origin.

The region in which any $x(0)$ can be driven back to the origin within two steps, denoted as Ω_r, is surrounded by two pairs of parallel lines: $x_1 + hx_2 = \pm h^2r$ and $x_1 + 2hx_2 = \pm h^2r$. As shown in Fig. 2, Ω_r is a parallelogram defined by the four points of $(-h^2r, 0)$, $(-3h^2r, 2hr)$, $(h^2r, 0)$ and $(3h^2r, -2hr)$.

Now, any initial state $M(x_1, x_2)$ on the $x_1 - x_2$ plane can be driven back to the origin in a minimum and finite number of steps according to the control signal sequence above. The complete DTOC law is described as follows:

Step 1: Set $z_1 = x_1 + \lambda h x_2$, $z_2 = z_1 + h x_2$, where $\lambda \in (0,1]$ is a tuning parameter to determine the different coordinates of x_A, x_C, and x_B. Here, we choose $\lambda = 1$. If $|z_1| > h^2 r$ or $|z_2| > h^2 r$, then $M(x_1, x_2)$ cannot be driven back to the origin within two steps, i.e., $M(x_1, x_2) \notin \Omega_r$, go to the next step; otherwise, go to **Step 5**;

Step 2: If the initial state $M(x_1, x_2)$ satisfies $x_1 x_2 \geq 0$ and $M(x_1, x_2) \notin \Omega_2 \cup \Omega$, then the control signal takes on $u = -r\,\text{sign}(x_1 + h x_2)$;

Step 3: Determine the boundary of the region Ω, i.e., x_A, x_C and x_B according to (11).

Step 4: If $|x_1| \geq x_B$, then the control signal takes on $u = -r\,\text{sign}(x_1)$; if $|x_1| \leq x_A$, then the control signal takes on $u = r\,\text{sign}(x_2)$;

Step 5: If $|x_1| \leq x_C$, then the control signal takes on $u = -r\alpha\,\text{sign}(x_2)$; otherwise $u = r\beta\,\text{sign}(x_2)$, where $\alpha = \frac{x_C - |x_1|}{x_C - x_A}$ and $\beta = \frac{|x_1| - x_C}{x_B - x_C}$;

Step 6: If the initial state $M(x_1, x_2) \in \Omega_r$, then the control signal takes on $u = -\frac{z_2}{h^2}$;

Step 7: The algorithm ends.

From the deduction above, the mathematical derivation of a closed-form DTOC as a function of x_1, x_2, r, and h, denoted by $u(k) = Fast(x_1(k), x_2(k), r, h, x_A, x_B, x_C)$, is obtained.

Remark 1: The DTOC law proposed by [12], [16] is essentially a non-linear boundary transformation that includes complex non-linear calculations. The control signal of our new law is determined by using piecewise linear function according to the relative positions of the initial state and the corresponding x-axis values for intersection points x_A, x_C. This allows the new law to have a simple structure.

Remark 2: For **Step 1** of the algorithm in Subsection B, choosing a different λ can result in different points x_A, x_C and x_B. However, the whole algorithm does not need to change.

For the given signal sequence $\{V(k), k = 0, 1, 2, ...\}$, we can construct the TD based on $Fast$ as follows [19], [20]:

$$\begin{cases} u(k) = Fast(x_1(k) - V(k), x_2(k), r_0, c_0 h, x_A, x_B, x_C) \\ x_1(k+1) = x_1(k) + h x_2(k) \\ x_2(k+1) = x_2(k) + h u(k), k = 0, 1, 2, ... \end{cases}$$
(16)

where r_0 is the quickness factor, c_0 is the filtering factor, and h is the sampling size.

III. STRUCTURE ANALYSIS AND FILTERING CHARACTERISTIC OF $Fast$

The approximate linear format of the proposed TD in (16) can be shown as follows if one properly selects parameter r:

$$\begin{pmatrix} x_1(k+1) \\ x_2(k+1) \end{pmatrix} = \begin{pmatrix} 1 - \frac{0.5}{c_0^2} & (1 - \frac{0.75}{c_0})h \\ -\frac{1}{c_0^2 h} & 1 - \frac{1.5}{c_0} \end{pmatrix} \begin{pmatrix} x_1(k) \\ x_2(k) \end{pmatrix}$$
$$+ \frac{1}{c_0^2 h} \begin{pmatrix} 1 \\ 0.5h \end{pmatrix} v(k).$$
(17)

For convenience, the above equation can be expressed as

$$x(k+1) = Gx(k) + \Gamma v(k), k = 0, 1, 2...$$
(18)

where $x(k) = [x_1(k), x_2(k)]^T$, and G, Γ are the corresponding matrices in (17). If we assume that the input signal $v(t) =$
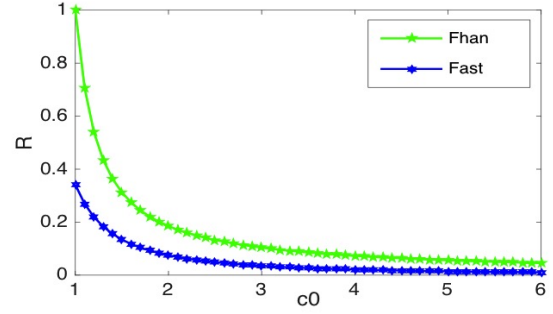

Fig. 3. Output variance sequence R vs filtering factor c_0.

$\sum_{i=1}^{N} A_i e^{j(w_i t + \phi_{i0})} + \xi(t)$, where $A_i, w_i \in \mathbf{R}^+$, $\phi_{i0} \in \mathbf{R}$ and $\xi(t)$ is a width-steady process. We have

$$x(k) = G^k p_0 + \sum_{i=1}^{N} (e^{j w_i h} I_2 - G)^{-1} \Gamma A_i e^{j(w_i k h + phi_{i0})} + \eta(k)$$
(19)

where $\eta(k+1) = G\eta(k) + \Gamma\xi(k)$, and p_0 is determined by initial condition $x(0)$ and $\eta(0)$. The necessary and sufficient condition for convergence for (19) is that the spectral radius of matrix G satisfies $\rho(G) < 1$. It can be derived that $x_1(k) = CG^k p_0 + \sum_{i=1}^{N} C(e^{j w_i h} I_2 - G)^{-1} \Gamma A_i e^{j(w_i k h + \phi_{i0})} + C\eta(k)$ by choosing $C = [1, 0]$. When the transfer function of the discrete time system is denoted as $\Phi(z) = C(z I_2 - G)^{-1} \Gamma$, $x_1(k)$ can be expressed as follows

$$x_1(k) = CG^k p_0 + \sum_{i=1}^{N} \Phi(e^{j w_i h}) A_i e^{j(w_i k h + \phi_{i0})} + C\eta(k).$$
(20)

For comparisons of filtering characteristics between $Fast$ and $Fhan$ algorithms, we only consider the width-steady random process. For a discrete-time linear tracking differentiator, width-steady input results in width-steady output. When the random input $\xi(t)$ is a white noise sequence, $R_\xi = Q\delta(\tau)$, where $\delta(\tau)$ is the Kronecker delta function [21], [22] and Q is the constant matrix. The variance matrix then satisfies the equation $R_\eta(k+1) = GR_\eta(k)G^T + \Gamma Q\Gamma^T$. When the constant k is large enough, $R_\eta(k)$ converges to the constant matrix, i.e.,

$$R_\eta = GR_\eta G^T + \Gamma Q\Gamma^T.$$
(21)

The above equation is a Lyapunov function of a discrete time system that presents the relationship between the output variance sequence R and the filtering factor c_0. For the algorithm $Fhan$, the matrix G and Γ are

$$G_1 = \begin{pmatrix} 1 & h \\ \frac{1}{c_0 h} & 1 - \frac{2}{c_0} \end{pmatrix}, \Gamma_1 = \begin{pmatrix} 0 \\ \frac{1}{c_0^2 h} \end{pmatrix}$$

respectively. Assume that the white-noise power spectrum density is $Q = 1$. Fig. 3 demonstrates the relationship between the output variance sequence R and the filtering factor c_0.

As shown in Fig. 3, choosing the proper filtering factor c_0 allows that the proposed TD based on the control law $Fast$ to effectively filter random noise. Compared with the control law $Fhan$, the $Fast$ algorithm performs better in signal-filtering.
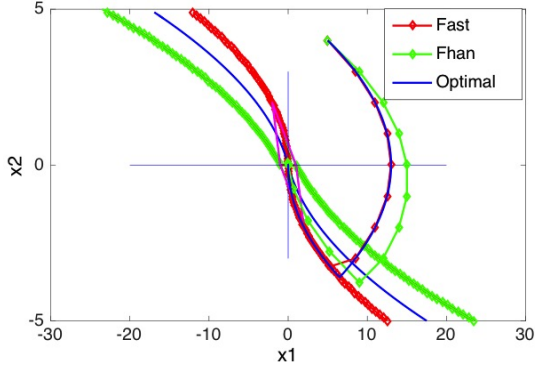
Fig. 4. Illustration of state trajectory under two different algorithms.

Fig. 5. Comparison of tracking errors between $Fhan$ and $Fast$ algorithms.

Fig. 6. Differentiation of signal errors compared between $Fhan$ and $Fast$ algorithms.

IV. SIMULATIONS AND EXPERIMENTS

By numerical simulations, we compare the state trajectory, signal-tracking, and differentiation of input signals between the algorithm $Fhan$ and the algorithm $Fast$. Furthermore, we compare the computation resources needed for two algorithms by the field-programmable gate array (FPGA) implementation. Experiments have also been conducted on signal processing for the position sensing in the speed and position detection system of a maglev train. Our objective is to show that using the proposed tracking differentiator to construct a tracking differentiator group with a moving-average algorithm can filter noise effectively, compensate for phase delays, and amend distortion signals at track joints, and it performs better than the algorithm $Fhan$.

A. Numerical Simulation

The switching curve function of the algorithm $Fhan$ is Γ_A: $x_1 + \frac{x_2|x_2|}{2r} + \frac{1}{2}hx_2 = 0$, while the switching curve function of TOC is $\Gamma_0 : x_1 + \frac{x_2|x_2|}{2r} = 0$. Fig. 4 illustrates the state trajectory under two different algorithms, $Fhan$ and $Fast$. We can see that the state trajectory for $Fast$ is in accordance with the optimal trajectory while the state trajectory for $Fast$ lags the optimal trajectory.

We then demonstrate the errors of tracking and differentiation of signals between the algorithms $Fhan$ and $Fast$. The Matlab program of Euler method is adopted in investigation. We choose the same initial value ($x_{10} = 0$, $x_{20} = 2$) and the input signal sequence $v(t) = \sin(2\pi t) + \gamma(t)$ in all simulations, where $\gamma(t)$ is the evenly distributed white noise with an intensity of 0.005. The sampling step is $h = 0.01$, the quickness factor is $r_0 = 100$, and the filtering factor is $c_0 = 1.5$.

The simulation results are plotted in Figs. 5 and 6. The algorithm $Fast$ quickly tracks an input signal without overshooting and chattering, while also obtaining an excellent differentiation of the input signal. This algorithm is more accurate in its tracking and differentiation compared with the other algorithm.

We introduce the FPGA to compare the computational resources needed between two algorithms. A great amount of multipliers and logic-element resources would be consumed
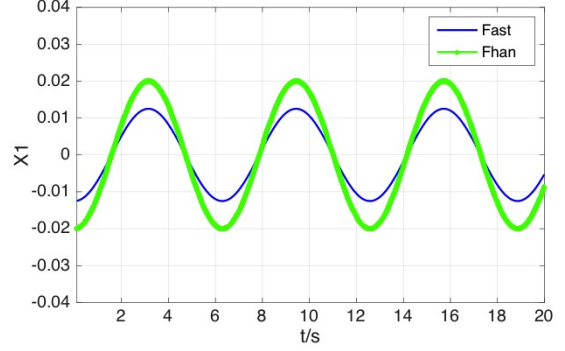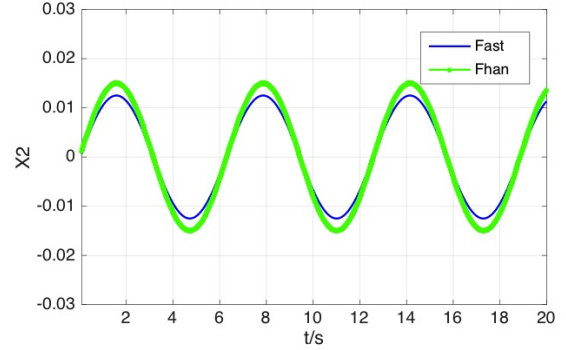
in FPGA implemented, in particular, for square root operations. For square root operations, the method of successive approximations by the VHDL language is used and the FPGA resources consumed are compared by single running of the two different algorithms in Table 1.

From Table 1, we see that the proposed $Fast$ algorithm significantly reduces the computation resources needed.

B. Experiment Validation

A permanent magnet electrodynamic suspension train uses a linear motion actuator to realize traction function [23], [24]. As shown in Fig. 7, the synchronous traction system comprises a speed and position detection system, a radio unit, a ground traction system, and a traction power module. The speed and position detection system is a core part of the synchronous traction system, which is used to receive and process the sensors' data. It sends the processed data of the speed and position of the train to the traction system in terms of the agreement to realize traction function. Therein, the position sensor can detect inductance changes of long stators' alveolar structures (see Fig. 7) to acquire the position information about the train.

In practice, the detection coils of the position sensor face long stators' alveolar structures. When the position sensor moves along the long stators, it can distinguish the teeth and the slots by detecting changes of inductance, and meanwhile,

TABLE I
COMPARISON OF THE COMPUTATION RESOURCES NEEDED IN FPGA BETWEEN $Fhan$ AND $Fast$

Algorithm	Multiplications	Square-root operations	Logic-Element (LE)	Clock cycles
$Fhan$ (32 bit)	14	1	290	74
$Fast$ (32 bit)	6	0	6	5

Fig. 7. Synchronous traction system.

Fig. 10. Illustration of TD group
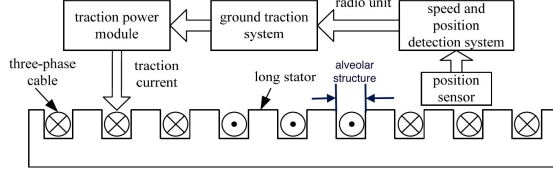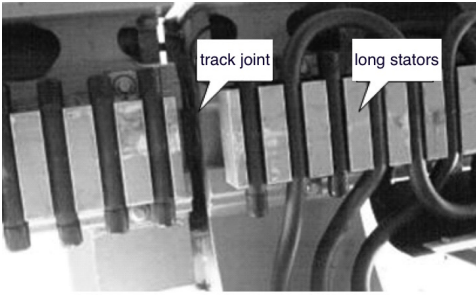
Fig. 8. Track joint in traction system.

Fig. 11. Results of magnetic pole phase filtering and phase compensation with the algorithm $Fast$ and $Fhan$.

the position of the train can be detected by counting the number of passed alveolar structures. Then, the position sensor transforms the position information into the output of the magnetic pole phase (from 0 to 60 degrees), where the phase signal between 0 to 60 degrees represents the length of one alveolar structure. Afterwards, the speed and position detection system processes the position data in accordance with the requirements of the traction system to compose the magnetic pole phase (from 0 to 360 degrees) for the traction.

For prevention of thermal expansion and contraction, the long stator track features numerous stators with many joints ($80mm$ of the actual displacement) along the track (see Fig. 8). These joints distort the outputs of the magnetic pole phase from the position sensors. The expected output of the position sensor when maglev train is passing over track joint is shown in Fig. 9. However, because of the track joints, the position signal will be more or less aberrant as the train passes.
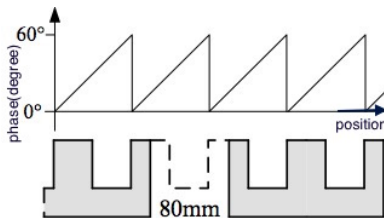

Fig. 9. The expected output of the position sensor when the maglev train passes over track joint.
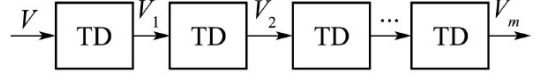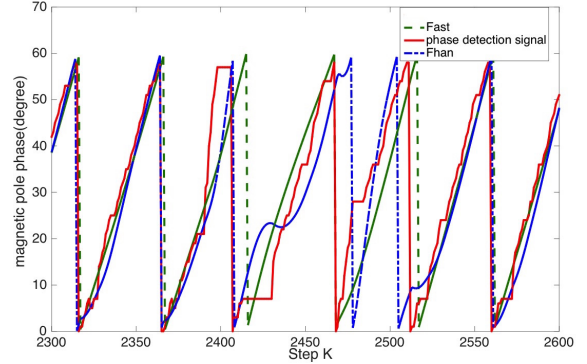
To amend the distortion of position signals at track joints, the TD based on algorithm $Fast$ is introduced. We use the proposed TD to construct the TD group (see Fig. 10), employing a moving-average algorithm to compensate for any phase delay. The moving-average algorithm is determined as

$$\hat{V}(t) = \sum_{k=1}^{n} C_n^k (-1)^{(k+1)} V_k(t) \tag{22}$$

We choose $n = 3$, leading to $\hat{V}(t) = 3V_1(t) - 3V_2(t) + V_3(t)$.

The experimental data are acquired from the speed and position detection system when the train is passing over a track joint. In the experiments, the parameters are set by the trial and error method as follows: for the algorithm $Fast$, the sampling step is $h = 0.005s$, the quickness factor is $r_0 = 100$, and the filtering factor is $c_0 = 40$, while for the algorithm $Fhan$, the sampling step is $h = 0.005s$, the quickness factor is $r_0 = 300$, and the filtering factor is $c_0 = 45$. Figure. 11 shows that, when the proposed TD group is used based on the algorithm $Fast$, the aberrant magnetic pole phase from the position sensor becomes smoother and the aberrant signal is greatly improved. The phase delay is small enough to meet the need of traction system. Furthermore, compared with the TD based on the algorithm $Fhan$, we can find that the TD based on $Fast$ is superior to the $Fhan$ in filtering and phase compensation. Such findings verify the effectiveness of the TD based on the $Fast$ algorithm.

V. Conclusion

In this brief, we proposed a novel second-order TD based on discrete time optimal control. The boundary curves and the control characteristic curve were obtained using the state backstepping method. Using the linearized criterion in control law allows us to obtain a new TD with a simple structure. The filtering mechanism was identified through structure analysis. Numerical simulation results showed that the TD based on the algorithm $Fast$ is more effective and has better performance in signal-tracking and differentiation acquisition than the algorithm $Fhan$. Furthermore, the computation resources needed in FPGA application is greatly reduced using the proposed $Fast$ algorithm. Experiments on the speed and position detection system in a maglev train verified the effectiveness of the TD based on the algorithm $Fast$ in signal-processing. Future investigations will include an analysis of the accuracy of proposed TD and examining the stability and convergence of the tracking differentiator.

Acknowledgement

References

[1] Levant, Arie, and Miki Livne, "Exact differentiation of signals with unbounded higher derivatives," *IEEE Trans. Autom. Control*, vol. 57, no. 4, pp. 1076-1080, 2012.

[2] Li, Yun, Kiam Heong Ang, and Gregory CY Chong, "Patents, software, and hardware for PID control: an overview and analysis of the current art," *IEEE Control Systems*, vol. 26, no. 1, pp. 42-54, 2006.

[3] Astrom, Karl Johan, and Tore Hagglund, "The future of PID control," *Control Eng. Pract.*, vol. 9, no. 11, pp. 1163-1175, 2001.

[4] Ang, Kiam Heong, Gregory Chong, and Yun Li, "PID control system analysis, design, and technology," *IEEE Trans. Control Syst. Technol*, vol. 13, no. 4, pp. 559-576, 2005.

[5] Li, Yun, Kiam Heong Ang, and Gregory CY Chong, "PID control system analysis and design," *IEEE Control Syst.*, vol. 26, no. 1, pp. 32-41, 2006.

[6] Dabroom, Ahmed M., and Hassan K. Khalil, "Discrete-time implementation of high-gain observers for numerical differentiation," *Int. J. Control*, vol. 72, no. 17, pp. 1523-1537, 1999.

[7] Ibrir, Salim. "Linear time-derivative trackers," *Automatica*, vol. 40, no. 3, pp. 397-405, 2004.

[8] Davila, Jorge, Leonid Fridman, and Arie Levant, "Second-order sliding-mode observer for mechanical systems," *IEEE Trans. Autom. Control*, vol. 50, no. 11, pp. 1785-1789, 2005.

[9] Levant, Arie, "Robust exact differentiation via sliding mode technique," *Automatica*, vol. 34, no. 3, pp. 379-384, 1998.

[10] Levant, Arie, "Higher-order sliding modes, differentiation and output-feedback control," *Int. J. Control*, vol. 76, no. 9, pp. 924-941, 2003.

[11] Wang, Xinhua, Zengqiang Chen, and Geng Yang, "Finite-time-convergent differentiator based on singular perturbation technique," *IEEE Trans. Autom. Control*, vol. 52, no. 9, pp. 1731-1737, 2007.

[12] Han, Jingqing, "From PID to active disturbance rejection control," *IEEE Trans. Ind. Electron.*, vol. 56, no. 3, pp. 1731-1737, 2009.

[13] Guo, Bao-Zhu, and Zhi-Liang Zhao, "Active Disturbance Rejection Control for Nonlinear Systems: An Introduction," *John Wiley and Sons*, 2016.

[14] Bellman, Richard, Irving Glicksberg, and Oliver Gross, "On the bang-bang control problem," *Quarterly of Applied Mathematics*, vol. 14, no. 1, pp. 11-18, 1956).

[15] Johnson, C. D., and W. M. Wonham, "Optimal bang-bang control with quadratic performance index," *Journal of Basic Engineering, Transactions of the ASME, Series D*, vol. 86, pp. 107-115, 1964.

[16] Gao, Zhiqiang, "On discrete time optimal control: A closed-form solution," *American Control Conference., 2004. Proceedings of the 2004*, vol. 1, 2004.

[17] MacLeod, C., and R. M. Goodall, "Frequency-shaping LQ control of Maglev suspension systems for optimal performance with deterministic and stochastic inputs," *IEE Proceedings-Control Theory and Applications*, vol. 143, no. 1, pp. 25-30, 1996

[18] Lee, Hyung-Woo, Ki-Chan Kim, and Ju Lee, "Review of maglev train technologies," *IEEE Trans. Magn.*, vol. 42, no. 7, pp. 1917-1925, 2006.

[19] Hehong Zhang, Yunde Xie, Gaoxi Xiao, and Chai Zhai, "Closed-Form Solution of Discrete Time Optimal Control and Its Convergence," *IET Control Theory Appl.*, DOI10.1049/iet-cta.2017.0749, November 2017.

[20] Guo, Bao-Zhu, and Zhi-Liang Zhao, "Weak convergence of nonlinear high-gain tracking differentiator," *IEEE Trans. Autom. Control*, vol. 58, no. 4, pp. 1074-1080, 2013.

[21] Fontana, Marco, and K. Alan Loper, "Kronecker function rings: a general approach," *Lecture Notes in Pure and Applied Mathematics*, pp. 189-206, 2001.

[22] Zoubir, Abdelhak M., and B. Boashash, "The bootstrap and its application in signal processing," *IEEE Signal Processing Mag.*, vol. 15, no. 1, pp. 56-76, 1998.

[23] Hehong Zhang, Yunde Xie, and Zhiqiang Long, "Fault detection based on tracking differentiator applied on the suspension system of maglev train," *Mathematical Problems in Engineering*, 2015.

[24] Goodall, Roger M, "Dynamics and control requirements for ems maglev suspensions," *Proceedings of the 18th International Conference on Magnetically Levitated Systems and Linear Drives (MAGLEV 2004), Shanghai*, pp. 926-934, 26-28 October 2004.